A Laser Radar based on a "Impulse-like" Laser Diode Transmitter and a 2D SPAD/TDC receiver

Jaakko Huikari, Sahba Jahromi, Jussi-Pekka Jansson, Juha Kostamovaara
University of Oulu, Faculty of Information Technology and Electrical Engineering
Circuits and Systems Research Group
Oulu, Finland
jmth@ee.oulu.fi

***Abstract*—A pulsed TOF laser radar has been implemented and its performance characterized. The transmitter applies a QW double-heterostructure laser diode producing 0.6 nJ/ 100 ps laser pulses at the central wavelength of ~ 817 nm. The detector is a single-chip IC, manufactured in the standard 0.35 µm HV CMOS process, including a 9x9 SPAD array and a 10-channel TDC circuit. Both the SPAD array and the TDC circuit support a time gating feature allowing photon detection only to occur within a predefined time window. The SPAD array also supports the sub-array selection feature in order to respond to the laser spot wandering effect due to paraxial optics. A sub-array is a 3x3 SPAD array freely chosen within a 9x9 SPAD array. The characteristic measurement results demonstrate the measurement range of tens of meters with a linearity precision +/- 0.5 mm to the 11% target reflectivity and at pulsing frequency of 100 kHz. The distance dependent detection rate varies from 28% to 500%, thus providing a high measurement rate. The single-shot precision is ~ 20 mm. The deteriorating impact of high-level background radiation conditions on the SNR has been demonstrated as well as a scheme to improve it by detector time gating.**

Keywords—laser ranging; pulsed time-of-flight laser radar; SPAD array; sub-nanosecond laser pulse; Time-to-Digital converter

I. INTRODUCTION

Time-of-flight (TOF) laser radar techniques have been widely used for distance measurement applications such as the measurement of material level in containers, profiling and scanning of objects, in traffic safety applications such as collision avoidance, speed measurement and traffic control, and in positioning, surveying and docking, for example. One important advantage of optical radars over microwave radars is the easy collimation of optical beams with lenses. Due to the much shorter wavelength, the diffraction limited spot size is also much smaller (λ/D) and thus the spatial resolution of the measurement can be high, typically at the level of a few millimeters or centimeters only [1, 2].

Optical radars utilize typically either the pulsed TOF or the phase comparison techniques based on a continuous wave (CW) laser source [3]. Both techniques have successfully been applied in a wide variety of industries. In this paper we utilize the pulsed TOF principle in which the transit time of a short laser pulse from the transmitter to the object and then back to the receiver is measured with a time-to-digital converter (event-detection based timing) from which the target distance can be calculated based on the known speed of light. Fig. 1 shows the block diagram of the TOF laser radar system. The main advantage of this approach over the CW based techniques is that a high precision can be achieved in a wide operation range even with a single laser shot [4]. Typically, a pulsed TOF laser radar utilizes either a PIN or an avalanche photo diode (APD) as the photodetector, and the receiver works in the linear mode. In this mode the receiver produces a voltage signal that is in principle proportional to the current pulse of the photodetector (and thus to the envelope of the optical echo). The electrical receiver noise is in this case the key parameter limiting the sensitivity of the radar. Thus the realization of the wide-band receiver with low noise and wide dynamic range is a key challenge in the design of this kind pulsed time-of-flight laser radars [5].

In this work, instead of using the well-established linear receiving techniques for echo detection, we utilize single photon detection receiver techniques realized with a CMOS based 2D single-photon detector array. A single-photon avalanche diode (SPAD) is a pn-junction reverse-biased above its breakdown-voltage. A photon absorption induced electron-hole pair within depletion region may cause a fast accumulating avalanche breakdown. A consequential current surge through the pn-junction has a ps-scale jitter in relation to induced photon incident [6, 7]. By doing this, the receiver complexity can be markedly reduced even with improved sensitivity. Since now the single-shot precision is determined by the laser pulse width as a first order approximation, we also shorten the laser pulse from the typical 3…4 ns width to ~ 100 ps by utilizing enhanced gain switching in a specially designed quantum well double heterostructure (QW DH) laser diode [8]. The electronics of the whole radar including the transmitter, receiver and the time interval measurement unit is constructed onto a single printed circuit board. The key feature of this

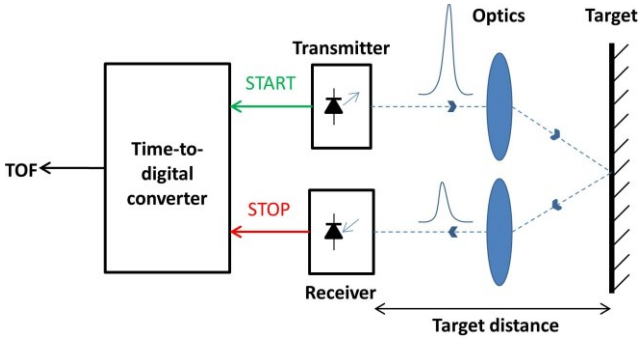

Fig. 1. TOF laser radar system.

Academy of Finland (Centre of Excellence in Laser Scanning Research, contract no. 272196, and contract nos. 255359, 283075 and 251571); Finnish Funding Agency for Innovation (TEKES).

realization in addition to compact size and the powerful sub-nanosecond pulse laser diode transmitter is the 2D CMOS SPAD detector. Such detector enables simultaneously low tolerance in the mechanical adjustments, the wandering of the laser spot on the surface of the detector along the object distance (a property of paraxial optics), and provides narrow optical field of view (FOV) matched with the FOV of the transmitter. The latter feature is essential in minimizing the background induced noise in the receiver [4].

II. Implementation

A. General view

The miniature radar realized in this work is a compact 1D pulsed TOF laser radar of high integration level. The transmitter and the receiver electronics have been implemented on a single printed circuit board (PCB) of 3.5 cm by 4.0 cm in size so that the distance between the laser diode and the detector IC is ~ 20 mm. The transmitter consist of a laser diode capable of producing high power and high speed laser pulses using a relatively simple pulsing scheme of a high-speed MOS-switch driving an RLC-circuit [9]. The detector, including the 2D 9x9 SPAD array and the 10-channel Time-to-Digital converter (TDC) circuit, is a single-chip IC manufactured in a standard 0.35 µm high voltage complementary metal-oxide-semiconductor (HV CMOS) process having the total chip dimensions of 2.5 mm x 4 mm [10]. Fig. 2 shows the photograph of the miniature laser radar laboratory setup in which the transmitter-receiver module is emphasized by a red circle. The photograph in Fig. 3 shows the dimension of the transmitter-receiver PCB and the locations of the laser diode and the detector IC. The detector IC outline is sketched by a yellow dashed line on a stray light cover.

B. Transmitter

The transmitter applies a QW double-heterostructure laser diode, an active stripe width and a cavity length of 30 µm and 3.0 mm, respectively. The laser diode operates in the enhanced gain-switching mode, based on the application of large equivalent spot size d_a/Γ_a, thus capable of producing nanojoule and 100 ps FWHM scale laser pulses [8]. The central wavelength of the laser emission is 817 nm. The transmitter electronics also includes TDC start pulse generation capability marking the time stamp of the moment of laser pulse emission.

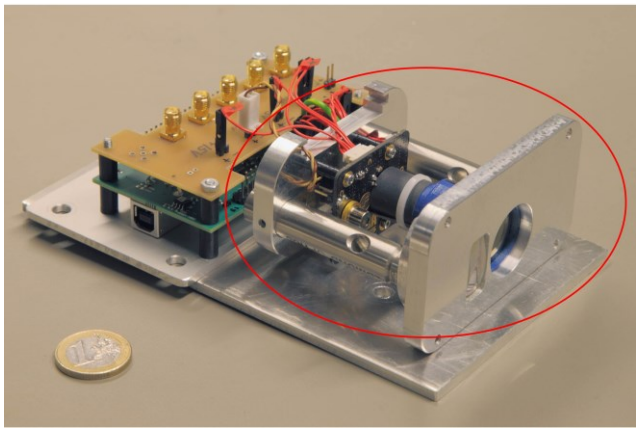

Fig. 2. Miniature laser radar.

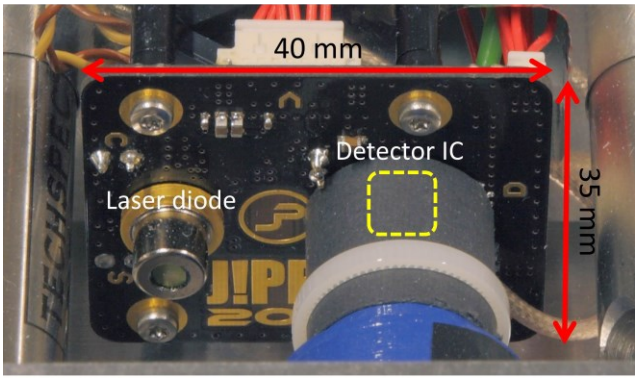

Fig. 3. Transmitter-receiver PCB.

In this work a drive current pulse amplitude of 4 A and FWHM of 1 ns were used to produce a laser pulse with energy and FWHM of 0.6 nJ and 100 ps, respectively. The pulsing frequency was 100 kHz.

C. SPAD array

The detector IC contains a 2D SPAD array as a photodetector element. The photon detection efficiency of a single SPAD element is approximately 5 – 2% at the wavelength range of 800 - 900 nm. The SPAD elements also have high photon detection timing precision, a typical jitter value in the order of ~ 80 ps, which corresponds well with the laser pulse width thus defining the single-shot precision in the order of 150 ps [4]. The 9x9 SPAD array is divided into 49 pieces of selectable sub-arrays (3 x 3 elements in each) which are controlling nine TCD stop channels. The selectable sub-array feature allows laser spot tracking due to the paraxial spot wandering. All SPAD elements share common quench and load signals but the selection signals are separate and determine which of the SPAD elements are loaded for photon detection. Each SPAD element also has a self-quench mechanism to bring the photon detection induced breakdown current to zero after a photon detection incident. The SPAD elements selected can be time-gated. In other words, it is possible to set the SPADs for photon detection for a user-defined time window only in relation to the start signal. The time gate window setting resolution is ~ 4 ns. The total SPAD array dimensions are 330 µm x 330 µm of which a single SPAD size is 24 µm x 24 µm. The SPAD array active area fill factor is around 50% [10].

D. TDC circuit

The detector IC also contains a 10-channel TDC circuit. Its operation principle is based on a counter and two interpolators. The TDC measures time intervals between a laser drive current pulse generated start signal and nine separate SPAD triggering induced stop signals. The maximum time range which the TDC is capable of measuring is ~ 533 ns (equivalent to ~ 80 m in distance) with single-shot precision of 10 ps. The TDC also supports the time gating feature allowing stop signal registering after a certain time interval after the start signal only. Finally, the TDC measured TOF time interval data, 18 bytes per each measurement, are transmitted to a PC by a FPGA board, which also handles the detector IC configuration in the beginning of the TOF measurement [10, 11].

E. Optics

Both the transmitter and the receiver apply achromatic lenses with 40 mm focal length and 20 mm in diameter. The transmitter lens width was ground to 9 mm in order to decrease the paraxial optics angle. See the photograph of laser radar optics in Fig. 4. The receiver's optical path also includes a bandpass filter, the center wavelength of 800 nm and the bandwidth of 50 nm, in order to decrease background radiation induced SPAD detections, i.e. noise. The transmitter beam divergence is 0.75 mrad and that of the receiver, defined by the whole 9x9 SPAD array area, is 8.25 mrad. For an individual SPAD element the divergence is 0.6 mrad. The transmitter was focused to 10 m and the receiver to infinity.

III. Measurements and Results

The first measurement was carried out to define linearity, signal detection rate, single-shot precision and target distance dependent behavior of the laser spot image on the surface of the SPAD array. The TOF measurement data was accumulated at 18 different target distances varying from 1 m to 34 m. The measurements were performed using a calibrated automated linearity measurement track with the target locating accuracy estimate of +/- 0.3 mm. The total amount of laser pulses applied per each measurement distance was 560 000. The detector gate window was opened ~ 25 ns before the target and the reflectance of the target was ~ 11%. The background radiation level during the measurements was < 50 lx (normal laboratory conditions). The laser radar was located minus ~ 45 cm offset from the linearity measurement track origin.

Next, the walk error measurement was performed to quantify how the distance measurement result systematically depends on a received signal power level. The higher the received signal level, the faster the avalanche builds up and, consequently, the closer the target appears to the distance measurement system. The less energetic phenomena taking place at the rising edge of the laser pulse, spontaneous emission and super luminescence, also become more visible to the receiver. The optical power reflected from the target to the receiver is dependent on the target surface material. The reflection coefficient of natural surfaces typically varies between 0.1 - 1. A reflection from a diffuse surface is dependent also on the cosine of the angle between the surface normal and the optical axis [12]. Three different kinds of target reflectivity values were used to alter the received signal level. The target materials used and their reflectivity values were, black rubber (4%) and white copy paper (100%) and highly directional diamond grade reflector (>> 100%).

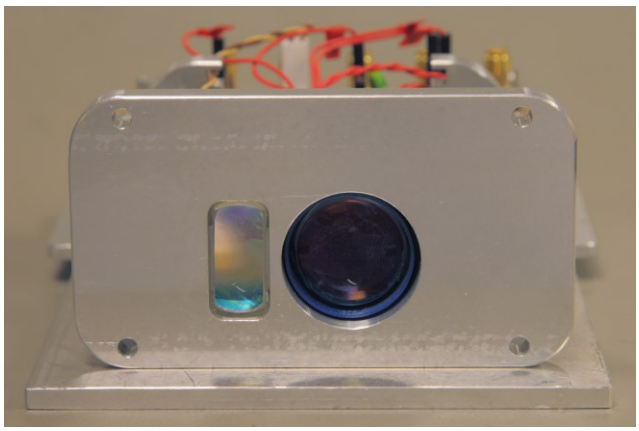

Fig. 4. Transmitter and receiver lenses.

The third, the photodetector time gating measurements were performed in high-level background radiation conditions, to determine the signal detection rate dependence on applied time gate window opening width before the target. The detector time gating can be applied to improve the photodetector's ability to see the signal photons from the target at high background radiation conditions. The measurement was performed outdoors around noon in order to maximize background radiation level. The sky was clear during the measurement and background radiation level was 90 klx. In total, ten different gate width values were applied ranging from 7.7 ns to 220 ns. The target was at 34 m and its reflectance coefficient was ~ 16%. Lastly, similar detector time gating measurement was performed when the target was at 73.2 m, applying only two extreme gate width values. Here the target is virtually at the edge of the laser radar reach, set by TDC circuit, thus offering an ultimate test for its performance.

A. Linearity

Fig. 5 illustrates the deviation of weighted average TOF measurement points from the least squares fitted reference line. The weighted TOF was defined by the mean TOF value of peak bin and its four neighbor bins, two bins on both sides. The mean value is calculated by weighted TOFs of nine SPADs defined by the selected 3x3 sub-array. The least squares fitted reference line was based on weighted TOF average values from 6 m to 34 m. The measured linearity is +/- 0.5 mm. The distinct decrease in weighted average TOF values at shorter distances is due to the increasing walk error caused by higher received energy from the target. The kink between one- and two-meter results is due to the laser spot finally dropping off of the SPAD array. This shift is due to the triangular geometry of the optical path of the laser pulse (paraxial optics) and its effect is becoming clearer at short distances, finally resulting in the spot to leave the SPAD array.

B. Detection Rate

Fig. 6 shows the combined 3x3 SPAD array signal detection rate vs. target distance. The exponential dependence of detection rate on distance (r) is in accordance with the

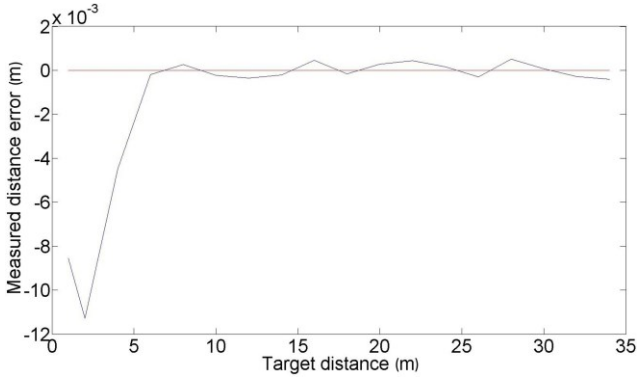

Fig. 5. Linearity error vs. target distance.

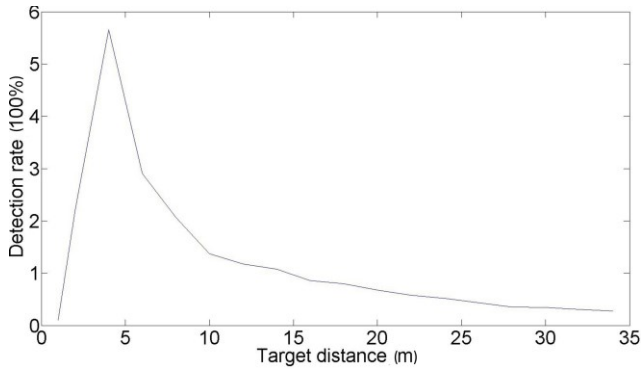

Fig. 6. Detection rate vs. target distance.

$1/r^2$ law. At short distances of one and two meters, though, the detection rate collapses due to spot wandering off of the SPAD array area, as explained above. Note the signal detection rates above 100% which are due to adding up nine separate signal detection rates of the SPAD elements.

C. Single-shot Precision

In Fig. 7 and Fig. 8 are two histograms of the single SPAD with the highest detection rate at two different target distances 4 m and 34 m. The FWHM of the histograms, based on the TDC bin width of 65 ps, is 130 ps, corresponding the single-shot precision of ~ 2 cm. Note the subtle change in the shape of the histogram which is caused by the response dependence of detector elements on the received power level making the trailing edge steeper at higher power, i.e. the target at a shorter distance. The signal detection rates are 95% and 10%, respectively.

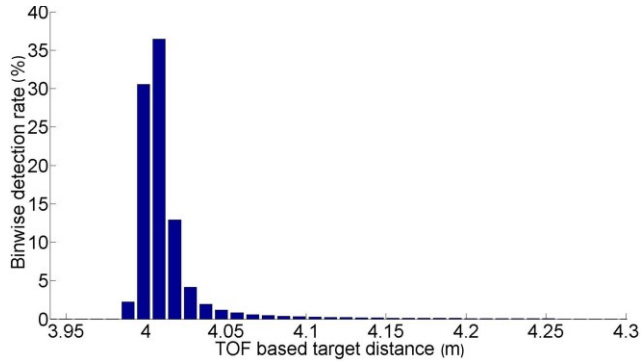

Fig. 7. Binwise detection rate, the target at 4 m.

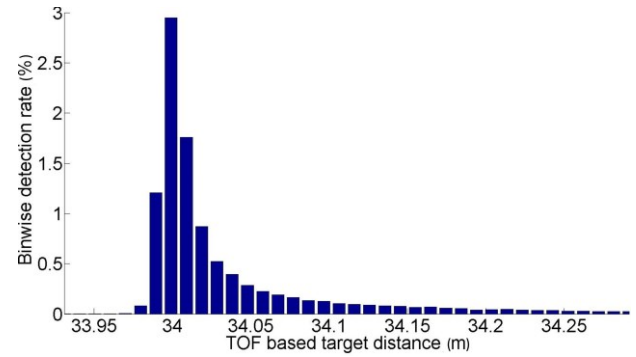

Fig. 8. Binwise detection rate, the target at 34 m.

D. Laser Spot Image on SPAD array

The series of 3D sketches in Fig. 9, representing the energy distributions of the laser spot image on the 9x9 SPAD array, illustrates the size of the image spot and its location on the SPAD array at six different target distances. The Y-axis represents the signal detection rate value. At the distances of 2 m and 4 m, the spot size increases and its location simultaneously shifts to the left, i.e. away from the transmitter. The spot size increase is due to the transmitter defocus and the spot shift due to paraxial optics. As visible from the sketches, the spot wandering also has coarse target distance information. Note also background radiation and especially dark count induced detections becoming visible as SNR decreases, while the target distance is increasing but also at one meter when the laser spot has left the SPAD array.

E. Walk error

The three TOF histograms in Fig. 10 are from the single SPAD with the highest signal detection rate. The advancing shift of the histogram peak location to the left, between black rubber and diamond grade, results in a walk error of ~ 5 cm.

F. Detector Behavior in High-Level Background Radiation Conditions

Fig. 11 shows the curve of the combined signal detection rate vs. total gate window opening length before the target at 34 m. The red dashed line is a reference signal detection rate value, ~ 28%, which was measured in low-level background radiation conditions of < 50 lx. The signal detection curve shows, for example, that at a 53 ns gate opening width the signal detection rate is ~ 5%. If the gate opening width is 24 ns instead, the signal detection rate increases to ~ 13%. The TOF histograms in Fig. 12 and Fig. 13 illustrate histogram development between wide and narrow gate window opening length. Note the exponentially decaying background radiation induced detection distribution in Fig. 12 and also the target with a low signal detection rate. The histograms in Fig. 14 and Fig. 15 show a similar development when the target was at 73.2 m. Now, in Fig. 14, the target is totally invisible to the laser radar due to background radiation blocking the detector, whereas in Fig. 15 the target becomes obvious.

IV. Discussion and Conclusion

The analysis and measurement results above demonstrate the feasibility and the distance measurement performance of the implemented miniature 1D laser radar. The transmitter produces high-power and high-speed laser pulses using a QW laser diode driven by a relatively simple drive current pulser scheme. The detector is a single-chip IC including a 9x9 SPAD array and a 10-channel TDC circuit. This configuration enables high-speed (100 kHz pulsing frequency) and high-precision (~ 2 cm single-shot precision) distance measurement results in addition to relaxed optomechanical accuracy requirements of the laser radar system. The laser diode and the receiver IC are located on a single compact PCB in the distance of ~ 20 mm from each other, thus making the overall size of the transmitter-receiver module relatively compact. Yet, regardless of the close proximity, the photon detector electronics appear, due to their digital-like nature, to be immune to the interference

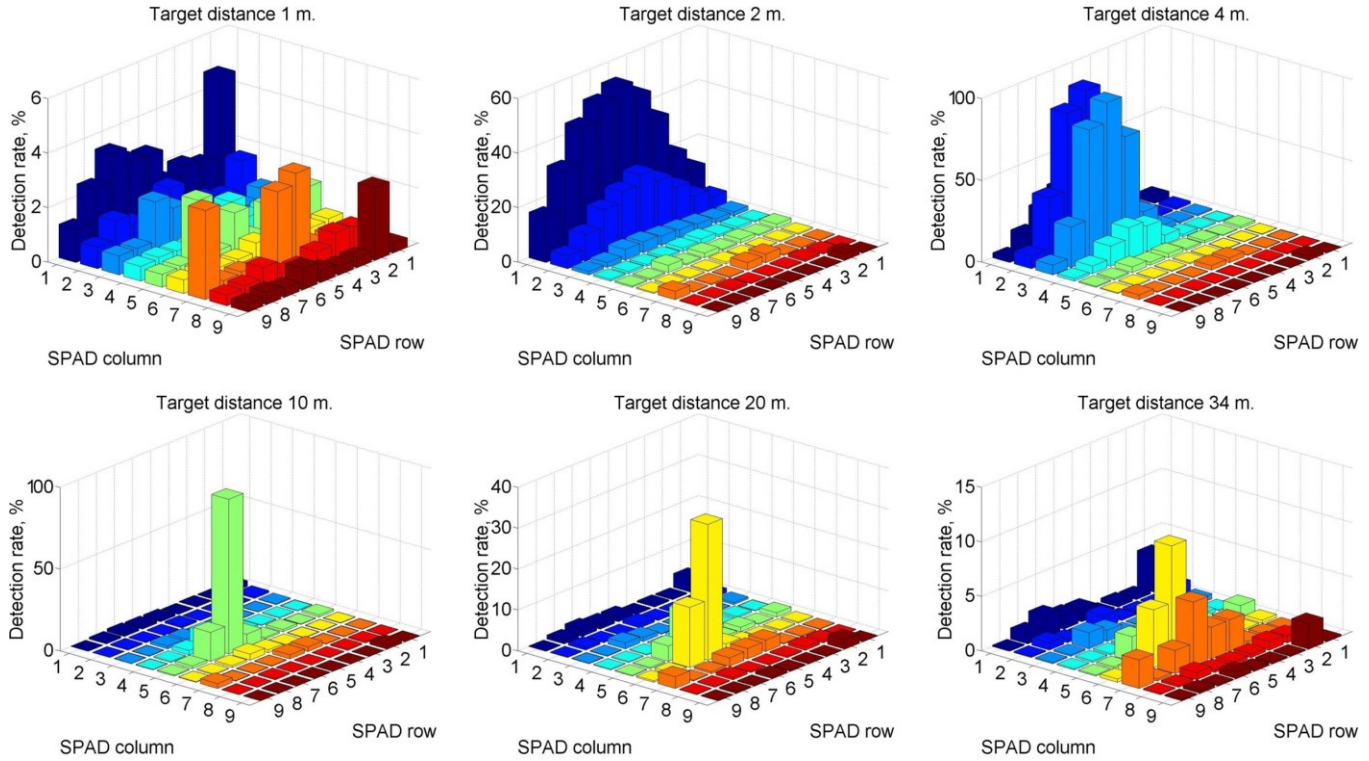

Fig. 9. Laser spot image's energy distribution on the 9x9 SPAD array.

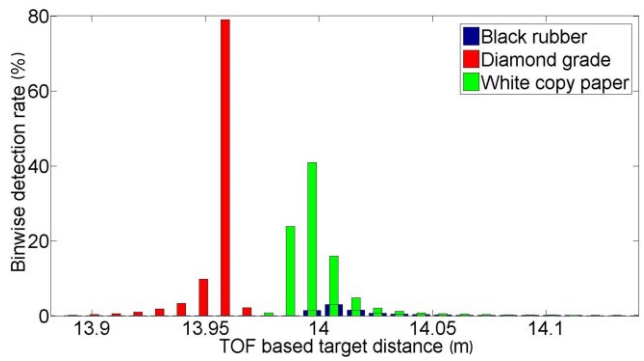

Fig. 10. Walk error.

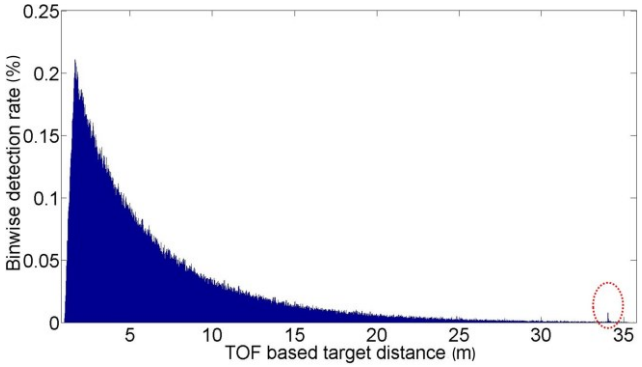

Fig. 12. Binwise detection rate, the target at 34 m. The wide time gate.

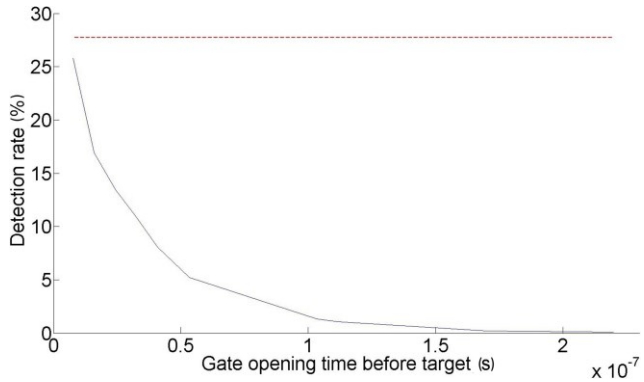

Fig. 11. Detection rate vs. gate opening time before the target.

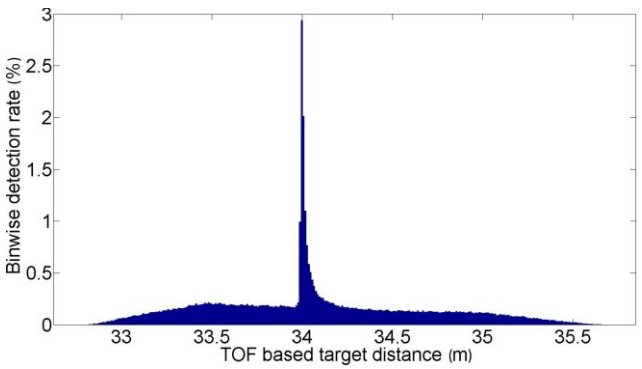

Fig. 13. Binwise detection rate, the target at 34 m. The narrow time gate.

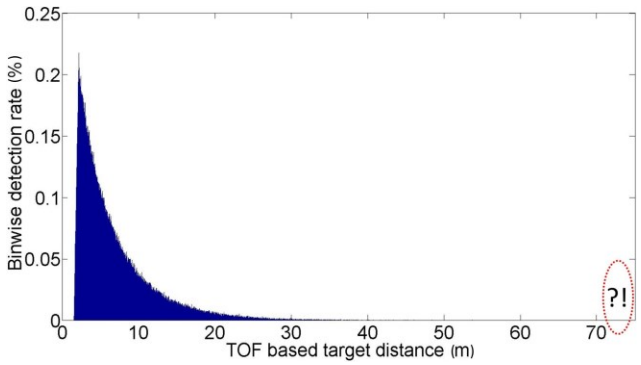

Fig. 14. Binwise detection rate, the target at 73.2 m. The wide time gate.

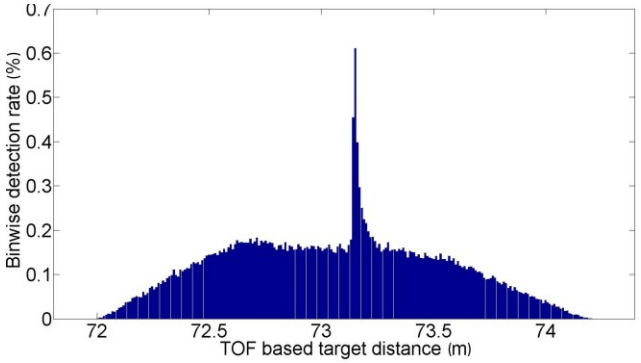

Fig. 15. Binwise detection rate, the target at 73.2 m. The narrow time gate.

caused by quite significant laser diode drive current pulse. The concept of SPAD array was introduced to allow for a target distance dependent laser spot wandering. This in conjunction with the selectable sub-array feature, according to a laser spot location, can be used to reduce background detections taking into account laser spot induced detections only.

REFERENCES

[1] M. Xuesong, D. Inoue, S. Kato, and M. Kagami, "Amplitude-modulated laser radar for range and speed measurement in car applications," IEEE Trans. Intell. Transp. Syst., vol. 13, no. 1, pp. 408–413, Mar. 2012.

[2] D. C. Carmer and L. M. Peterson, "Laser radar in robotics," Proc. IEEE, vol. 84, no. 2, pp. 299–320, Feb. 1996.

[3] S. Donati, Electro-Optical Instrumentation: Sensing and Measuring With Lasers. Upper Saddle River, NJ, USA: Prentice-Hall, 2004.

[4] J. Kostamovaara, et al., "On laser ranging based on high speed/energy laser diode pulses and single photon detection techniques", IEEE Photonics Journal, vol. 7, iss. 2, Apr. 2015, pp. 1-15.

[5] S. Kurtti and J. Kostamovaara, "An integrated laser radar receiver channel utilizing a time-domain walk error compensation scheme", IEEE Trans. on Inst. and Meas. (TIM), vol. 60, pp. 146-157.

[6] C. Niclass, et al., "Design and characterization of a 256x64-pixel single-photon imager in CMOS for a MEMS-based laser scanning time-of-flight sensor", Optics Express, vol. 20, iss. 11, pp. 11863-11881, 2012.

[7] K. Ito, et al., "System Design and Performance Characterization of a MEMS-Based Laser Scanning Time-of-Flight Sensor Based on a 256\times 64-pixel Single-Photon Imager", IEEE Photonics Journal, vol.5, no. 2, pp. 559-572, 2013.

[8] Huikari, J.M.T.; Avrutin, E.A.; Ryvkin, B.S.; Nissinen, J.J.; Kostamovaara, J.T., "High-Energy Picosecond Pulse Generation by Gain Switching in Asymmetric Waveguide Structure Multiple Quantum Well Lasers," Selected Topics in Quantum Electronics, IEEE Journal of, vol.21, no.6, pp.1,6, Nov.-Dec. 2015.

[9] J. Nissinen, and J . Kostamovaara, "A 4 a peak current and 2 ns pulse width CMOS laser diode driver for high measurement rate applications", ESSCIRC, 2013 Proceedings of the. IEEE, 2013.

[10] S. Jahromi, J. Jansson, I. Nissinen, J. Nissinen, and J. Kostamovaara, "A Single Chip Laser Radar Receiver with a 9x9 SPAD Detector Array and a 10-Channel TDC", ESSCIRC 2015-41st, pp. 364-367. IEEE, 2015.

[11] J. Jansson, A. Mantyniemi, and J. Kostamovaara, "A CMOS time-to-digital converter with better than 10 ps single-shot precision", IEEE J. Solid-State Circuits, vol. 41, pp. 1286-1296, Jun. 2006.

[12] D. C. O'Shea, Elements of modern optical design. John Wiley & Sons, Inc. United States of America, 1985.